Oncogene (2014) **33,** 3561–3570

www.nature.com/onc

ORIGINAL ARTICLE

PTRF/cavin-1 neutralizes non-caveolar caveolin-1 microdomains in prostate cancer

H Moon[1], CS Lee[2,3], KL Inder[1], S Sharma[2,3], E Choi[1,4], DM Black[1], K-A Lê Cao[5], C Winterford[6], JI Coward[7], MT Ling[8], the Australian Prostate Cancer BioResource, DJ Craik[9], RG Parton[9], PJ Russell[8] and MM Hill[1]

Caveolin-1 has a complex role in prostate cancer and has been suggested to be a potential biomarker and therapeutic target. As mature caveolin-1 resides in caveolae, invaginated lipid raft domains at the plasma membrane, caveolae have been suggested as a tumor-promoting signaling platform in prostate cancer. However, caveola formation requires both caveolin-1 and cavin-1 (also known as PTRF; polymerase I and transcript release factor). Here, we examined the expression of cavin-1 in prostate epithelia and stroma using tissue microarray including normal, non-malignant and malignant prostate tissues. We found that caveolin-1 was induced without the presence of cavin-1 in advanced prostate carcinoma, an expression pattern mirrored in the PC-3 cell line. In contrast, normal prostate epithelia expressed neither caveolin-1 nor cavin-1, while prostate stroma highly expressed both caveolin-1 and cavin-1. Utilizing PC-3 cells as a suitable model for caveolin-1-positive advanced prostate cancer, we found that cavin-1 expression in PC-3 cells inhibits anchorage-independent growth, and reduces *in vivo* tumor growth and metastasis in an orthotopic prostate cancer xenograft mouse model. The expression of α-smooth muscle actin in stroma along with interleukin-6 (IL-6) in cancer cells was also decreased in tumors of mice bearing PC-3-cavin-1 tumor cells. To determine whether cavin-1 acts by neutralizing caveolin-1, we expressed cavin-1 in caveolin-1-negative prostate cancer LNCaP and 22Rv1 cells. Caveolin-1 but not cavin-1 expression increased anchorage-independent growth in LNCaP and 22Rv1 cells. Cavin-1 co-expression reversed caveolin-1 effects in caveolin-1-positive LNCaP cells. Taken together, these results suggest that caveolin-1 in advanced prostate cancer is present outside of caveolae, because of the lack of cavin-1 expression. Cavin-1 expression attenuates the effects of non-caveolar caveolin-1 microdomains partly via reduced IL-6 microenvironmental function. With circulating caveolin-1 as a potential biomarker for advanced prostate cancer, identification of the molecular pathways affected by cavin-1 could provide novel therapeutic targets.

Oncogene (2014) **33,** 3561–3570; doi:10.1038/onc.2013.315; published online 12 August 2013

Keywords: PTRF; cavin-1; caveolin-1; caveolae; prostate cancer

INTRODUCTION

Caveolin-1 expression mediates the progression through the castration-resistant phase of prostate cancer by promoting Akt-mediated cell survival,[1] enhancing androgen-regulated cell cycle progression[2] and via paracrine actions of secreted caveolin-1.[3,4] Owing to its bioactive circulating form, caveolin-1 has been suggested as a clinically relevant biomarker for high-grade prostate cancer[5] and disease recurrence.[4,6] Furthermore, anti-caveolin-1 antibodies to neutralize circulating caveolin-1 have been suggested as potential therapy in prostate cancer.[7]

As caveolin-1 is an essential structural component of plasma membrane caveolae, cholesterol-rich-invaginated pits at the plasma membrane,[8] it has been assumed that caveolin-1 in prostate cancer cells forms caveolae. However, we recently demonstrated that the caveolin-1-positive prostate cancer cell line PC-3 lacks caveolae because of the absence of an essential co-factor cavin-1 (also known as PTRF; polymerase I and transcript release factor).[9] Caveolin-1 in PC-3 cells reside on flat plasma membrane as visualized by electron microscopy, but exhibits the same detergent-resistant property as caveolae, reflecting its partition to cholesterol-rich lipid raft membrane microdomains.[9] To distinguish the planar lipid raft structural organization from caveolae, we term such tumor-promoting caveolin-1 conformation non-caveolar caveolin-1. Ectopic expression of cavin-1 in PC-3 cells stabilizes the caveolin-1 protein and induces caveola formation,[9] concomitant with reduction in cellular migration.[10,11] Our cellular and proteomics studies revealed a potential molecular mechanism in that cavin-1 induced cholesterol re-distribution and reduction in the secretion of a subset of oncogenesis-related proteins such as proteases and cytokines.[12] These results suggest distinct roles of caveolin-1 and cavin-1 in prostate cancer cells.

To date, only one study examined the expression of cavin-1 in prostate cancer, with the finding that cavin-1 is reduced or absent in prostate cancer tissues ($n = 21$) but showed positive immunoreactivity in benign prostatic hyperplasia (BPH; $n = 17$).[13] Hence, this study sought to clarify the relative expression of caveolin-1

[1]The University of Queensland Diamantina Institute, The University of Queensland, Brisbane, Queensland, Australia; [2]Discipline of Pathology, School of Medicine and Molecular Medicine Research Group, University of Western Sydney, Sydney, New South Wales, Australia; [3]Department of Anatomical Pathology, Liverpool Hospital, Sydney, New South Wales, Australia; [4]School of Veterinary Science, The University of Queensland, Brisbane, Queensland, Australia; [5]Queensland Facility for Advanced Bioinformatics, The University of Queensland, Brisbane, Queensland, Australia; [6]School of Medicine, The University of Queensland, Brisbane, Queensland, Australia; [7]Mater Research, Translational Research Institute, Brisbane, Queensland, Australia; [8]Australian Prostate Cancer Research Centre–Queensland and Institute for Biomedical Health & Innovation, Queensland University of Technology, Translational Research Institute, Brisbane, Queensland, Australia and [9]Institute for Molecular Bioscience, The University of Queensland, Brisbane, Queensland, Australia. Correspondence: Dr MM Hill, The University of Queensland Diamantina Institute, The University of Queensland, Level 5, Translational Research Institute, 37 Kent Street, Woolloongabba, Brisbane 4102, Australia.
E-mail: m.hill2@uq.edu.au
Received 5 February 2013; revised 8 June 2013; accepted 11 June 2013; published online 12 August 2013

and cavin-1 in normal, non-malignant and malignant patient tissues, and to determine relative roles of caveolae versus non-caveolar caveolin-1 microdomains, by modulating cavin-1 co-expression in prostate cancer cells.

RESULTS

Expression of caveolin-1 and cavin-1 in prostate tissues

We generated a rabbit polyclonal antibody against the N-terminal 15 amino acids of human cavin-1. Following affinity purification against the antigenic peptide, the specificity of the antibody was confirmed by immunoblotting with lysates from several previously characterized cell lines in Hill *et al.*[9] To investigate the expression of caveolin-1 and cavin-1 in prostate tissues, we performed immunohistochemistry on two tissue microarrays (TMAs) from the Australian Prostate Cancer BioResource. The normal prostate tissue array was designed to show age-related histological changes, and contained 2 to 3 cores from 141 prostate cancer-free participants with age range from 15 to 79 (mean 37.5) years. The Gleason-graded TMA contained cores from 117 patients with Gleason scores 4–9 with matching non-malignant tissue (adjacent normal and BPH). The mean patient age for the Gleason grade TMA was 63 (range 52–74) years. Semiquantitative assessment of the immunostaining for caveolin-1 and cavin-1 was performed independently by two pathologists (C Soon Lee and Sowmya Sharma) using a scoring system, where a score of 2 indicates strong staining in $>30\%$ of tissue, a score of 1 indicates diffuse staining or strong staining in $<30\%$ of tissue and score 0 indicates no staining. Interobserver variation was seen in $<1\%$ of the cases (14 of the tissue cores) and any discrepant results were reassessed by both pathologists simultaneously at a multiheader microscope and a consensus result was then obtained. As the loss of caveolin-1 in prostate stroma has been proposed as a marker of metastatic progression,[14] the stroma compartment (Table 2) was scored separately from the epithelia/carcinoma (Table 1). Consensus scores were categorized in contingency tables, with scores 1 and 2 categorized as 'positive' and score 0 as 'negative'.

In total, 258 participants were assessed for caveolin-1 and cavin-1 expression. The previously reported upregulation of caveolin-1 in advanced prostate carcinoma[15–17] was replicated in our study cohort (Figure 1a and Table 1; $P<0.0001$). Endothelial cells of blood vessels served as internal positive controls, having high expression of caveolin-1 and cavin-1 (Figure 1; black arrow head). Analysis of the TMA results showed a lack of cavin-1 expression in normal as well as malignant prostate epithelia (Figure 1b and Table 1), indicating that caveolin-1 in prostate cancer (epithelial compartment) is present in non-caveolar microdomains. On the other hand, normal prostate stroma highly expressed both caveolin-1 and cavin-1, which was significantly reduced in malignant stroma (Table 2; $P<0.0001$). The loss of stromal caveolin-1 and cavin-1 expression significantly correlated with Gleason score (Table 2; $P<0.0001$). Loss of stromal caveolin-1 has been correlated with elevated prostate cancer caveolin-1,[14] therefore we went on to examine the correlation between epithelial caveolin-1 and stroma cavin-1. Caveolin-1 is most prevalent in the high-risk (Gleason score $\geqslant 8$) group, with 75% of the patients showing positivity (Table 1). In this group, stromal caveolin-1 and cavin-1 was lost in 35% and 53%, respectively, suggesting that epithelial caveolin-1 expression leads to loss of stromal caveolin-1 and cavin-1 (and loss of caveolae structure). This is in agreement with the observation for stromal caveolin-1

Table 1. The expression of caveolin-1 and cavin-1 in normal, non-malignant and malignant prostate epithelia

	Caveolin-1 (*P < *0.0001*)			*Cavin-1* (P = *0.1350*)		
	Total	*Negative*	*Positive*	*Total*	*Negative*	*Positive*
Non-cancer normal	128	123 (96.1%)	5 (3.9%)	141	141 (100.0%)	0 (0.0%)
BPH	49	45 (91.8%)	4 (8.2%)	50	50 (100.0%)	0 (0.0%)
Cancer						
Gleason score $\leqslant 6$	66	44 (66.7%)	22 (33.3%)	66	65 (98.5%)	1 (1.5%)
Gleason score $= 7$	31	14 (45.2%)	17 (54.8%)	31	30 (96.8%)	1 (3.2%)
Gleason score $\geqslant 8$	20	5 (25.0%)	15 (75.0%)	20	20 (100.0%)	0 (0.0%)

Test used: χ^2-test for trend. *Significance <0.0001. Healthy normal specimens were biopsy cores from men with no history of prostate diseases and other cancers. Benign prostatic hyperplasia (BPH) specimens were cores from a prostate cancer progression tissue microarray. Prostate cancer samples were further classified by Gleason scores: a score of 6 or less: low risk; a score of 7: moderate risk; a score of 8 or more: high-risk prostate cancer.

Table 2. The expression of caveolin-1 and cavin-1 in prostate stroma

	Caveolin-1 (*P < *0.0001*)			*Cavin-1* (*P < *0.0001*)		
	Total	*Negative*	*Positive*	*Total*	*Negative*	*Positive*
Non-cancer normal	124	0 (0.0%)	124 (100.0%)	133	2 (1.5%)	131 (98.5%)
BPH	49	1 (2.0%)	48 (98.0%)	49	0 (0.0%)	49 (100.0%)
Cancer						
Gleason score $\leqslant 6$	65	8 (12.3%)	57 (87.7%)	65	16 (24.6%)	49 (75.4%)
Gleason score $= 7$	31	13 (41.9%)	18 (58.1%)	31	9 (29.0%)	22 (71.0%)
Gleason score $\geqslant 8$	17	6 (35.3%)	11 (64.7%)	17	9 (52.9%)	8 (48.0%)

Test used: χ^2-test for trend. *Significance <0.0001. Peri-epithelial stroma defined as stroma in 10 cell layers from the epithelia has been examined. Non-cancer normal specimens were from men with no prostate diseases, and benign prostatic hyperplasia (BPH) specimens were from a prostate cancer progression tissue microarray. Prostate cancer samples were further classified by Gleason scores: A score of 6 or less: low risk; a score of 7: moderate risk; a score of 8 or more: high-risk prostate cancer.

by Di Vizio *et al.*[14] However, a direct causal relationship remains to be confirmed. In this study, we focused on the tumor-promoting actions of non-caveolar caveolin-1 and modulation by cavin-1.

Cavin-1 co-expression suppressed PC-3 tumor progression and metastasis

To identify and generate suitable cell models for investigation of non-caveolar caveolin-1, we examined the caveolin-1 and cavin-1 expression pattern in three commonly used prostate cancer cell lines, LNCaP, 22Rv1 and PC-3. Similar to the TMA results, all three cell lines lacked cavin-1 expression (Figure 2a). In contrast, caveolin-1 was detected in PC-3 cells, but not in LNCaP or 22Rv1 cells (Figure 2a). Previously, we reported that cavin-1 co-expression with caveolin-1 induced caveolae in PC-3 cells,[9] concomitant with reduced migration and membrane protrusion.[10,11] Here, we further show that cavin-1 overexpression significantly decreased cell growth and anchorage-independent growth of PC-3 cells (Figure 2b and c). In order to confirm these *in vitro* findings in an *in vivo* mouse model, we utilized a previously reported PC-3 luciferase cell line[18] and generated independent cell lines stably expressing cavin-1 or vector control (Supplementary Figure S1a). As the lentivirus expresses green fluorescent protein under a bi-cistronic promoter, we used flow cytometry to isolate 99% pure population of expressing cells. Cell proliferation and anchorage-independent growth were measured, and the PC-3 luciferase cell lines were confirmed to behave similarly to the original PC-3 cell lines (Supplementary Figure S1b). Before use in an orthotopic prostate cancer xenograft mouse model, we confirmed that the two cell lines showed similar linear intensities of *in vitro* bioluminescence correlating with cell number (Supplementary Figure S2). Half a million PC-3 cells were injected into dorsolateral prostate glands of non-obese diabetic-severe combined immunodeficient mice. Tumor progression and metastases were examined by *in vivo* and *ex vivo* bioluminescence imaging. PC-3-cavin-1 cells showed a significant reduction in tumor progression compared with control PC-3 cells (Figure 3a and b), and smaller size and weight of prostate tumors were confirmed by necropsy at the end of experiments (Figure 3c and d; $P = 0.0007$). *Ex vivo* bioluminescence imaging also revealed a significant reduction (15.2-fold reduction; $P = 0.0289$) of lung metastases in mice injected with PC-3-cavin-1 cells compared with PC-3 control (Figure 3e).

Cavin-1 co-expression reduced interleukin-6 (IL-6) and alpha-smooth muscle actin (α-SMA) in prostate tumor and stroma in PC-3 xenografts

To determine *in vivo* tumor cell proliferation, formalin-fixed paraffin-embedded sections were stained for Ki-67 (Figure 4a). The number of Ki-67-positive cells was quantified by two researchers independently counting cells at five different

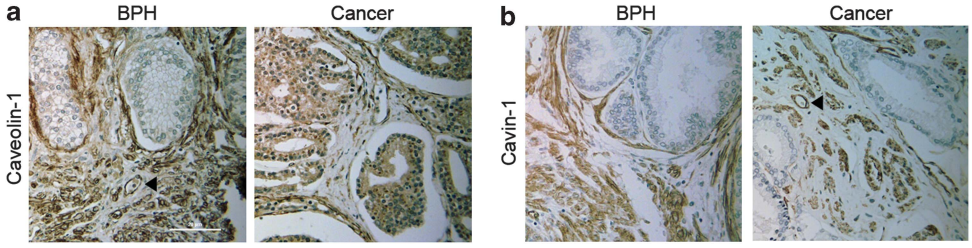

Figure 1. Immunohistochemistry staining of caveolin-1 and cavin-1 in prostate tissues. (**a**) Representative figures of caveolin-1 immunoreactivity in BPH and prostate cancer specimens. (**b**) Representative figures of cavin-1 immunoreactivity in BPH and prostate cancer specimens. Endothelial cells of blood vessels (black arrow head) served as an internal positive control for caveolin-1 and cavin-1. Bar: 20 μm, × 200.

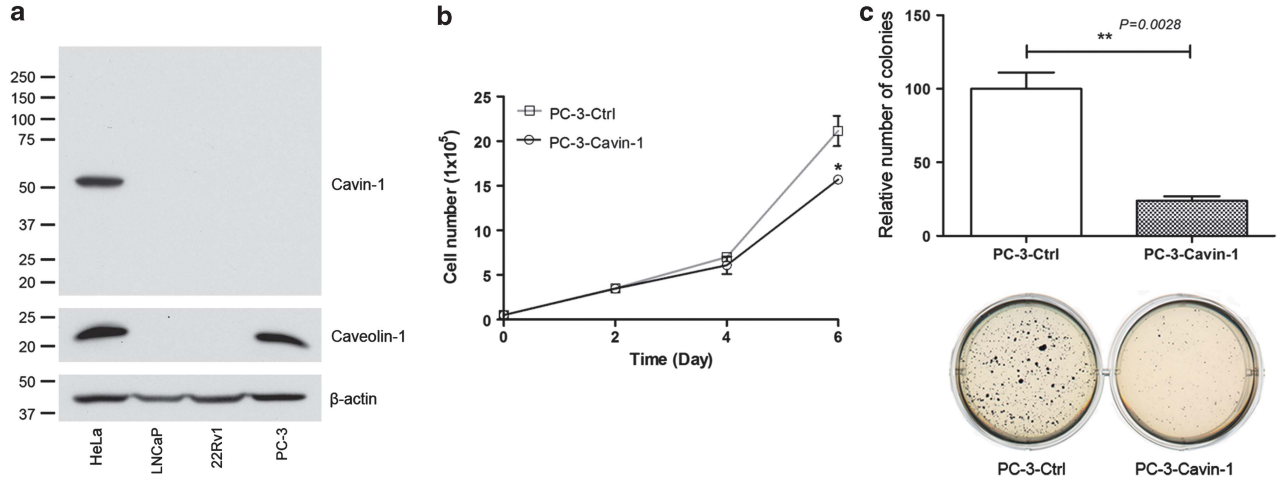

Figure 2. Cavin-1 and caveolin-1 expression in prostate cancer cell lines, and effects of cavin-1 co-expression in caveolin-1-positive prostate cancer PC-3 cells. (**a**) Expression of caveolin-1 and cavin-1 in prostate cancer cell lines. Total cell lysates (20 μg) from HeLa, LNCaP, 22Rv1 and PC-3 cells were separated on sodium dodecyl sulfate–polyacrylamide gel electrophoresis (SDS–PAGE) and immunoblotted with cavin-1, caveolin-1 and β-actin as indicated. Cavin-1 antibody detected a single band in HeLa cell lysate. Representative of at least three independent experiments. (**b**) Growth curve of PC-3 cell lines. Cell numbers were determined at the indicated days, and values represent mean ± s.e.m. of three independent experiments performed in quadruplicates (*$P < 0.05$). (**c**) Anchorage-independent growth assay of PC-3 cell lines. A total of 10 000 cells were seeded in medium with soft agar in six-well plates and cultured at 37 °C for 21 days. Experiments were repeated four times (**$P < 0.005$).

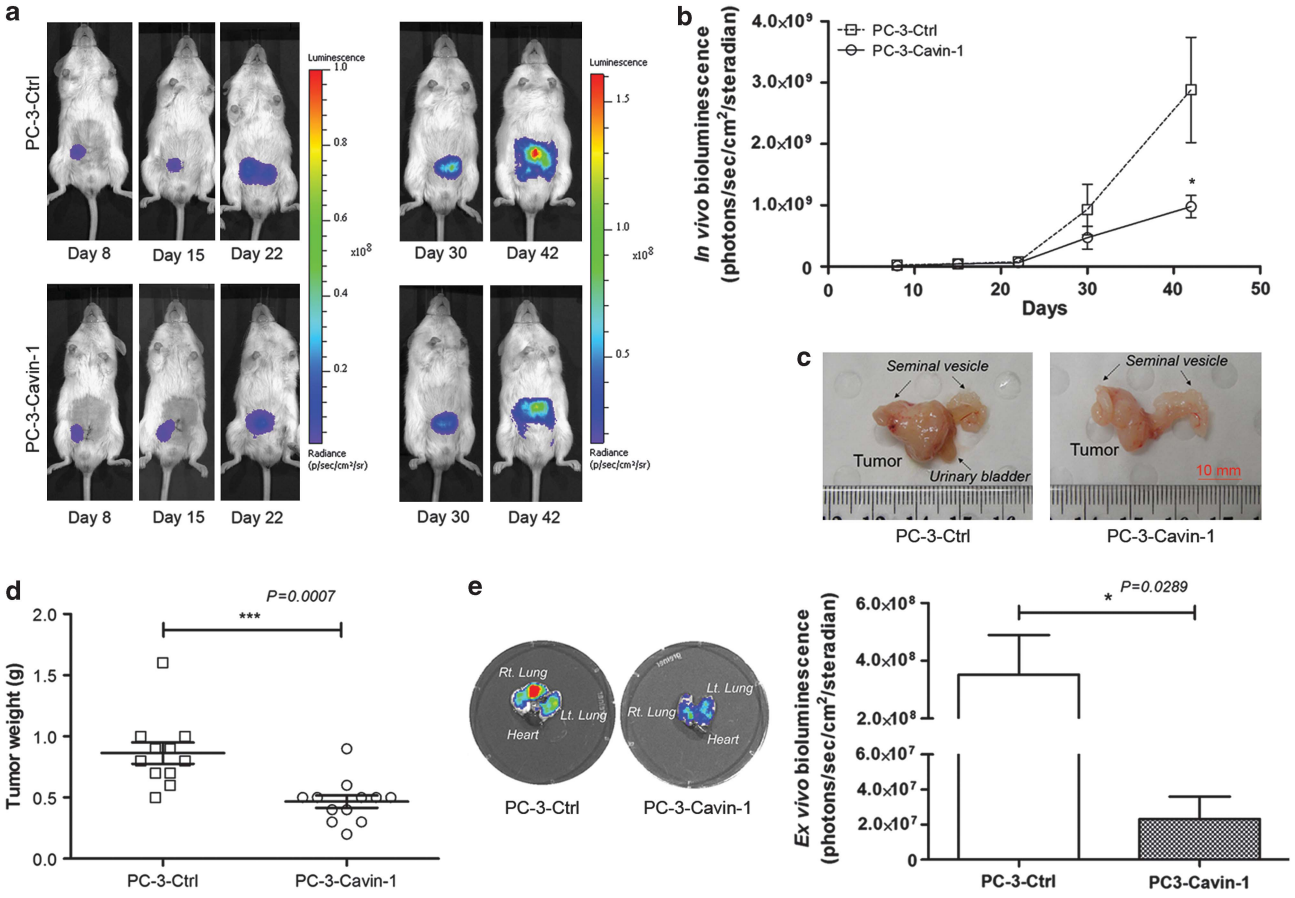

Figure 3. Effects of cavin-1 co-expression on PC-3 tumor growth and metastasis. (**a**) Representative figures of whole-body bioluminescence imaging in non-obese diabetic-severe combined immunodeficient (NOD/SCID) mice. The dorsolateral prostate glands of male NOD/SCID mice were injected with 5×10^5 PC-3 cells in 25 μl PBS, and tumors were imaged at the indicated days. Before imaging, D-luciferin dissolved in PBS was intraperitoneally injected. (**b**) Prostate tumor growth was compared between PC-3 control and PC-3-cavin-1 by the intensity of bioluminescence at the region of interest. Six randomly selected mice per group were imaged on the indicated days. At day 42, the bioluminescence of every mouse was monitored by the IVIS spectrum. Values represent mean ± s.e.m. ($*P<0.05$). (**c**) At the end of *in vivo* experiments, representative PC-3 control and PC-3-cavin-1 prostate tumors were collected and photographed. (**d**) Final prostate tumor burden was measured 6 weeks after injecting PC-3 tumor cells ($n=11$ for PC-3 control and 12 for PC-3-cavin-1, $***P<0.0005$). (**e**) *Ex vivo* imaging was performed with lung tissues excised from a subset of mice immediately after final *in vivo* imaging. The mean values of the intensity of bioluminescence in the lung tissues were >10 times higher in PC-3 control relative to PC-3-cavin-1 group ($*P<0.05$).

high-power fields per sample (Figure 4b). In agreement with the *in vivo* bioluminescence results, PC-3-cavin-1 tumor showed significantly reduced *in vivo* proliferation (Figure 4a and b; $P=0.0001$). Next, we examined the tumor tissues for IL-6 levels as a potential molecular mediator of the tumor-suppressing effect of cavin-1.

Our previous study using quantitative proteomics revealed that cavin-1 co-expression on PC-3 cells reduced the secretion of growth factors and proinflammatory cytokines including IL-6.[12] IL-6 has been implicated in prostate cancer progression,[19] particularly with gaining androgen independence.[20,21] Furthermore, anti-IL-6 monoclonal antibody has demonstrated effectiveness against castration-resistant prostate cancer.[21–23] As caveolin-1 is associated with androgen insensitivity,[24] attenuation of IL-6 may be a potential mechanism of the antitumor effect of cavin-1 expression in our PC-3 prostate tumor model. Staining of primary prostate tumor tissues with anti-human IL-6 antibodies revealed significantly reduced IL-6 expressions in PC-3-cavin-1 tumors compared with control tumors (Figure 4c and d; $P=0.0049$). Recently, IL-6 has been proposed to mediate the establishment of the tumor microenvironment by reciprocal interplay between stroma and cancer cells.[25–27] To examine if cavin-1 expression also affected the tumor microenvironment, we examined the expression of α-SMA, which is one of main activation markers for reactive stroma.[28] As seen in Figure 4e and f, α-SMA was reduced in stromal tissues in mice bearing PC-3-cavin-1 tumor cells ($P=0.0014$). These results suggest that cavin-1 expression attenuates PC-3 tumor progression, possibly via the IL-6 pathway and cross-talk between cancer and stromal cells.

Cavin-1 inhibits anchorage-independent growth in caveolin-1-positive LNCaP cells

Caveolin-1 is associated with the development of androgen independence.[29] Our previous studies examined cavin-1 function in androgen-independent prostate cancer cells and suggest that cavin-1 exerts both caveolin-1-dependent and -independent functions.[10,11] To determine if the same holds in androgen-sensitive prostate cancer cells, which do not express caveolin-1 (Figure 2), we generated 22Rv1 and LNCaP cell lines stably expressing caveolin-1 or cavin-1 using the same lentivirus system as above, and confirmed their expression by western blotting (Figure 5a). Cell proliferation and anchorage-independent growth was measured for these cell lines. In contrast to the PC-3 cells (Figure 2b), neither caveolin-1 nor cavin-1 overexpression altered cell proliferation in 22Rv1 or LNCaP cells (Figure 5b and c).

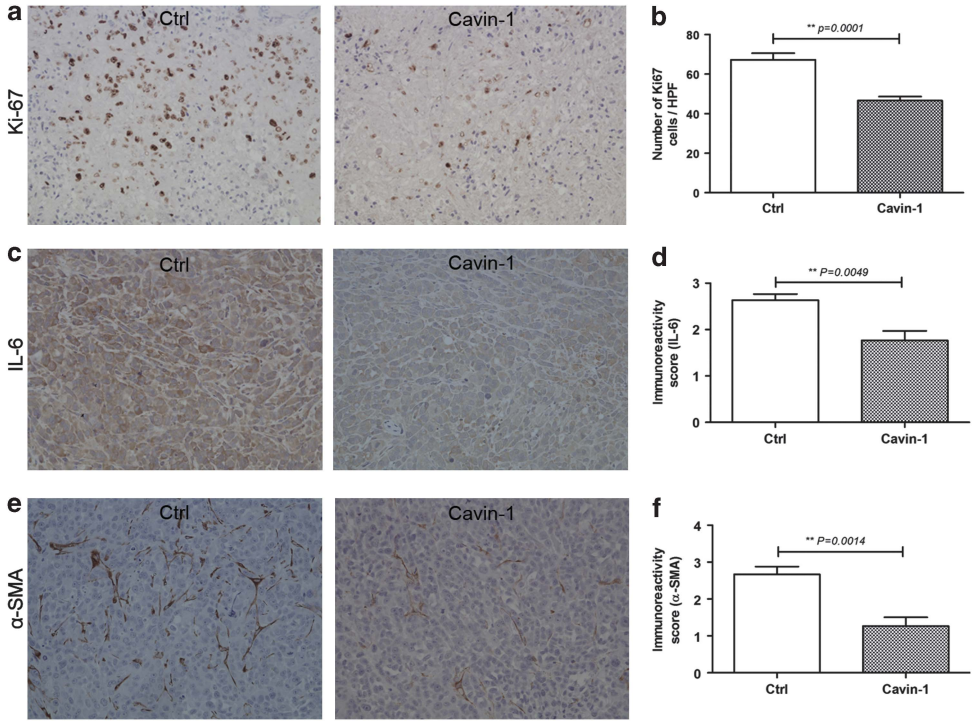

Figure 4. Cavin-1 co-expression affects proliferation and IL-6 expression of tumor cells, and α-SMA expression of stroma tissues. (**a**) Immunohistochemical Ki-67 staining of PC-3 control and PC-3-cavin-1 tumors for cell proliferation (original magnification, × 200). (**b**) The number of Ki-67-positive cells was counted in five randomly selected from each tumor ($n = 8$ per group) in high-power field (HPF). (**c**) Representative figures of IL-6 staining in PC-3 control and PC-3-cavin-1 tumors (× 200). (**d**) Semiquantitative scoring for IL-6 was assessed in five independent microscopic fields for each PC-3 control ($n = 6$) and PC-3-cavin-1 ($n = 6$) tumors. (**e**) Immunohistochemical staining of α-SMA in control and cavin-1 group (× 200) (**f**) α-SMA staining was semiquantitatively determined in five randomly selected fields from each tumor ($n = 6$ per group). All data were represented as mean ± s.e.m. with two independent observers (**$P < 0.005$).

However, caveolin-1 overexpression significantly accelerated colony formation in soft agar in both cell lines, while cavin-1 had no effect on anchorage-independent growth (Figure 5d and e). These results suggest that cavin-1 expression alone has no effect on tumor-promoting potential of caveolin-1-negative androgen-dependent prostate cancer cells.

Next, we examined if cavin-1 co-expression could reverse caveolin-1-induced anchorage-independent growth in LNCaP cells. Cavin-1 lentivirus was used to infect caveolin-1-expressing LNCaP cells. Expression levels were confirmed by immunoblotting (Figure 6a), and >95% of cells expressed cavin-1 as confirmed by immunofluorescence with cavin-1 antibody (data not shown). Confocal immunofluorescence using anti-caveolin-1 and cavin-1 antibodies showed colocalization to surface puncta suggesting caveola formation and localization (Figure 6b). Consistent with Figure 5b and c, cavin-1 expression had no effect on cell proliferation of LNCaP-caveolin-1 cells (Figure 6c). In contrast, cavin-1 co-expression in caveolin-1-positive LNCaP cells significantly inhibited anchorage-independent growth (Figure 6d). This set of experiments indicates that cavin-1 can neutralize the tumor-promoting effects of non-caveolar caveolin-1 but does not itself alter tumor-promoting potential of prostate cancer cells.

Cavin-1 co-expression neutralizes caveolin-1-mediated androgen receptor and IL-6 expression, and Akt phosphorylation

To further delineate the molecular pathways modulated by cavin-1, we examined three prostate cancer targets associated with caveolin-1, androgen receptor (AR),[30] IL-6 (Figure 4c and d) and phospho-Akt[1,31] using our LNCaP and PC-3 cell models. As shown in Figure 7a, caveolin-1 overexpression increased cellular levels of AR (1.69 ± 0.09, $P = 0.0034$) and IL-6 (1.89 ± 0.06, $P = 0.0066$) in LNCaP cells, whereas cavin-1 overexpression showed no significant changes of AR (1.11 ± 0.08, $P = 0.4657$) or IL-6 (1.32 ± 0.10, $P = 0.1424$). In agreement with a planar caveolin-1-neutralizing role, cavin-1 co-expression significantly decreased the expression of AR (1.15 ± 0.11, $P = 0.0227$) and IL-6 (1.17 ± 0.17, $P = 0.0086$) in LNCaP-caveolin-1 cells (Figure 7a). Previously, we reported reduced secretion of IL-6 from PC-3 cells upon cavin-1 overexpression.[12] Therefore, we also examined if the secretion of IL-6 from LNCaP cells was changed by either caveolin-1 or cavin-1 overexpresison. As a positive control, caveolin-1 was detected in the conditioned media of caveolin-1-positive cells (Figure 7b) as previously reported.[3] The secretion of caveolin-1 in LNCaP (Figure 7b; 1.08 ± 0.14) and PC-3[22] was not significantly altered upon cavin-1 overexpression. Previous studies consistently reported the expression of receptors for IL-6 in LNCaP cells, however, there have been conflicting results as to whether or not LNCaP cells secrete IL-6.[32–34] In this study, we found that neither caveolin-1 nor cavin-1 expression induced the secretion of IL-6 in LNCaP cells (Figure 7b), although cellular IL-6 levels were altered by overexpression of caveolin-1 or cavin-1 co-expression (Figure 7a).

Caveolin-1 has been reported to regulate cell signaling via phosphatidylinositol-3-kinase-Akt and Ras-extracellular signal-regulated kinase (ERK) pathways.[35] To determine if cavin-1 expression alters caveolin-1-mediated cell signaling, we examined the level of pAkt and pERK in cell extracts from caveolin-1-positive LNCaP and PC-3 cells. As shown in Figure 7c, cavin-1 overexpression specifically reduced the levels of phosphorylated Akt in LNCaP-caveolin-1 (0.71 ± 0.04. $P = 0.0048$) and PC-3 (0.68 ± 0.1, $P = 0.0482$) cells, without affecting ERK 1/2 phosphorylation.

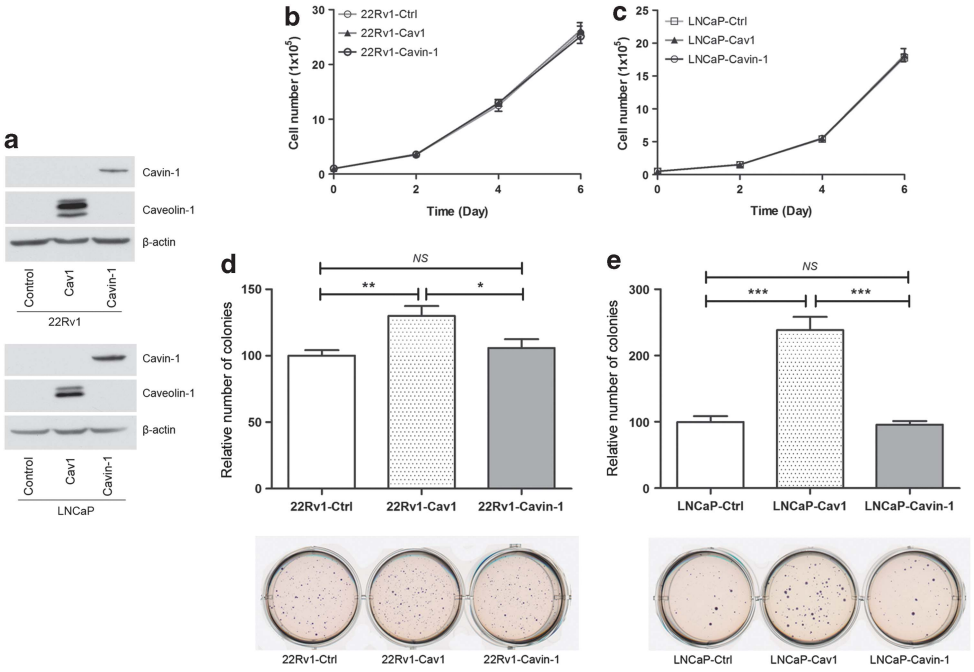

Figure 5. Differential effects of caveolin-1 and cavin-1 in prostate cancer 22Rv1 and LNCaP cells. (**a**) Total cell lysates (20 μg) from 22Rv1 and LNCaP stable cell lines expressing caveolin-1 or cavin-1 were separated on sodium dodecyl sulfate–polyacrylamide gel electrophoresis (SDS–PAGE) and immunoblotted with cavin-1, caveolin-1 and β-actin as indicated. (**b**) Growth curve of stable 22Rv1 cell lines. Cell numbers were determined at the indicated days, and values represent mean ± s.e.m. of three independent experiments performed in quadruplicates. (**c**) Growth curve of stable LNCaP cell lines was determined at the indicated days by counting cells. (**d**) Anchorage-independent growth assay of stable 22Rv1 cells. A total of 10 000 cells were plated in six-well plates between two layers of agarose, top layer being 0.35% and bottom layer 0.5%. Cells were incubated at 37 °C for 28 days. (**e**) Anchorage-independent growth of stable LNCaP cells was determined by colony formation in soft agar as above. LNCaP cells were incubated for 21 days. All experiments represented in this figure were repeated at least four times (*$P<0.05$, **$P<0.005$, ***$P<0.0005$). NS, not significant.

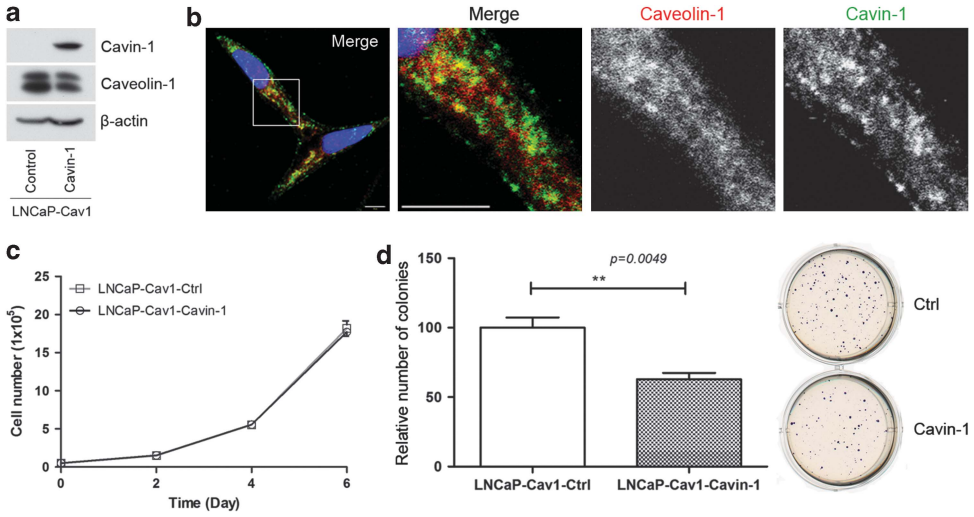

Figure 6. Cavin-1 co-expression in LNCaP-caveolin-1 cells suppresses anchorage-independent growth. (**a**) Expression level of cavin-1, caveolin-1 and β-actin was measured by immunoblotting total cell lysates (20 μg) from LNCaP-caveolin-1 as indicated. (**b**) Confocal immunofluorescence of LNCaP-caveolin-1-cavin-1 cells showing colocalization of caveolin-1 (red) and cavin-1 (pseudogreen). Bar, 20 μm. The nucleus was visualized with 4,6-diamidino-2-phenylindole (DAPI) staining (blue). (**c**) Growth curve of LNCaP-caveolin-1 cells expressing cavin-1 or control. Cell numbers were counted on the indicated days, and values represent mean ± s.e.m. of three independent experiments performed in quadruplicates. (**d**) Anchorage-independent growth assay of LNCaP-caveolin-1 with or without cavin-1 expression. A total of 10 000 cells were plated in six-well plates between two layers of agarose, top layer being 0.35% and bottom layer 0.5%. Cells were incubated at 37 °C for 21 days (**$P<0.005$).

DISCUSSION

Although caveolin-1 has been associated with aggressive prostate cancer since the 1990s, this is the first study to comprehensively demonstrate that caveolin-1 in the majority of prostate carcinoma is present in non-caveolar microdomains because of the lack of cavin-1 expression. We further show that cavin-1 expression attenuates PC-3 tumor progression *in vivo*, with microenvironmental modulation as a potential mechanism (Figure 8).

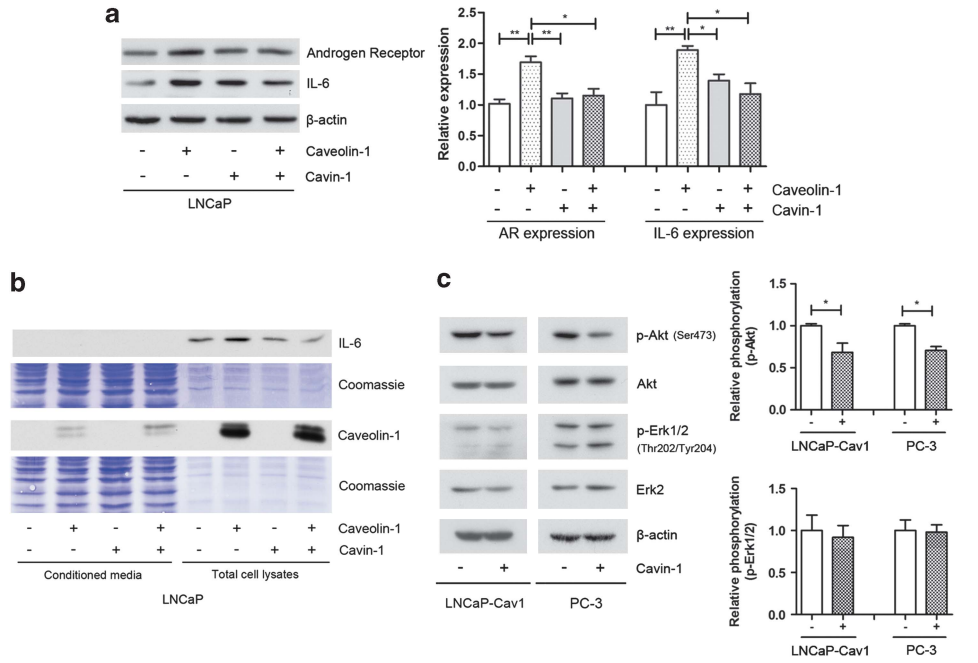

Figure 7. Cavin-1 co-expression negatively regulates AR, IL-6 and phospho-Akt. (**a**) Total cell lysates (20 μg) from LNCaP stable cell lines expressing caveolin-1 and/or cavin-1 were separated on sodium dodecyl sulfate–polyacrylamide gel electrophoresis (SDS–PAGE) and immunoblotted with AR and IL-6 as indicated. The relative intensity of western blot signals were quantified using Image J (National Institutes of Health, Bethesda, MD, USA), and the values are represented in the bar graph. (**b**) LNCaP stable cell lines were cultured in serum-free media for 24 h, and then conditioned media were collected. Conditioned media (25 μg) and total cell lysates (5 μg) were separated on SDS–PAGE and immunoblotted with IL-6 and caveolin-1 as indicated. Loading control: Coomassie staining. (**c**) Western blot analysis shows decrease of Akt but not Erk phosphorylation by cavin-1 co-expression in LNCaP-caveolin-1 and PC-3 cells. The relative phosphorylation is represented in bar graphs. All experiments represented in this figure were repeated at least three times (*$P<0.05$, **$P<0.005$).

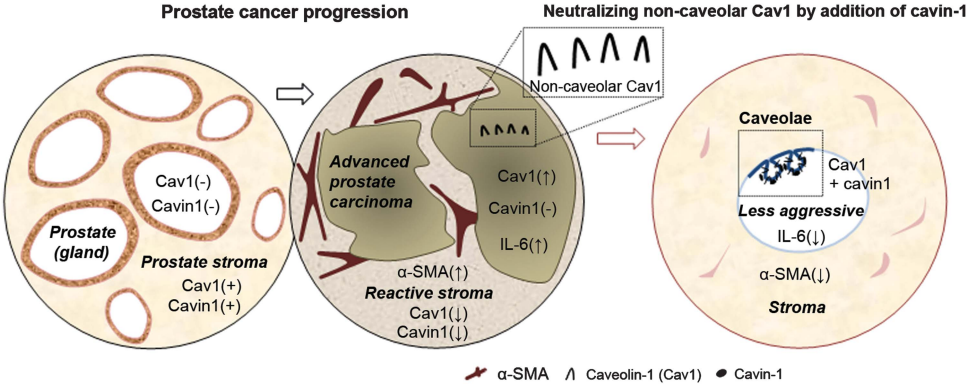

Figure 8. Working model of caveolin-1 and cavin-1 expressions in prostate cancer progression and the effect of cavin-1 co-expression in advanced prostate cancer. Normal and non-malignant prostate epithelia express neither caveolin-1 nor cavin-1, while normal prostate stroma highly expresses both caveolin-1 and cavin-1. Caveolin-1 but not cavin-1 (non-caveolar caveolin-1, inset) is upregulated in prostate cancer as Gleason score increases. On the other hand, stromal caveolin-1 and cavin-1 are downregulated in prostate cancer. Ectopic cavin-1 co-expression neutralizes tumor-promoting effects of caveolin-1 microdomains in prostate cancer cells through the reduction of IL-6 (cancer cells) and α-smooth muscle actin (α-SMA in stroma).

The tumor-suppressing effect of cavin-1 is dependent on the presence of non-caveolar caveolin-1, since expression of cavin-1 alone in LNCaP and 22Rv1 cells (caveolin-1-negative) did not affect anchorage-independent growth, but interfered with the tumor-promoting ability of planar caveolin-1. Cavin-1 co-expression also reversed the caveolin-1-induced elevation of AR and IL-6 expression in LNCaP cells, and specifically reduced pAkt without modulating pERK in LNCaP and PC-3 cells. Hence, investigating the molecular pathway modulated by cavin-1 will allow identification of novel therapeutic targets for caveolin-1-positive prostate cancer patients. Such a personalized treatment strategy is highly translatable to the clinic since circulating caveolin-1 is a ready minimally invasive biomarker to identify these high-risk patients.[36]

Other cavin family members, cavin-2 (serum deprivation-response protein, SDPR), cavin-3 (protein kinase C, delta binding protein, PRKCDBP, also known as SRBC) and cavin-4 (muscle-restricted coiled-coil protein, MURC), also have important roles in caveola functions.[37–39] Although few studies directly examine the role of cavin-2 and cavin-3 in cancer, several studies have identified downregulation of cavin-2 or cavin-3 via methylation in different cancers, including prostate.[40–43] These results are in agreement with our hypothesis of a tumor-promoting role for non-caveolar

caveolin-1, either because of loss of caveolae structure as in the case of reduced cavin-2 or cavin-3 expression, or because of aberrant expression of caveolin-1 in cells that do not express cavin-1, as in the case of PC-3 cells (Figure 8).

Although cavin-1 is absent in normal, non-malignant and malignant prostate epithelia in our cohort ($n = 258$ participants), Gould *et al.*[13] showed positive cavin-1 immunoreactivity in BPH ($n = 17$). Our cavin-1 immunohistochemistry quality was assured by the strong stromal cavin-1 staining and positivity of endothelial cells on the same slides. One possible explanation for the discrepancy is the different epitopes of the antibodies used. We generated a new polyclonal antibody to the N-terminal peptide of human cavin-1, while Gould *et al.*[13] used a commercial antibody generated using recombinant mouse cavin-1 protein comprising the middle region (amino acids 157–272). Hence, there is the intriguing possibility that proteolytic cleavage may regulate cavin-1 levels in prostate epithelium. Cavin-1 contains PEST sequences and has been reported to be proteolytically cleaved in adipocyte caveolae.[44] Whether cavin-1 cleavage occurs outside of caveolae, and its relevance in prostate cancer remains to be investigated.

A role for stromal caveolin-1 in remodeling of the microenvironment has been proposed,[45] although the mechanism underlying the differential function of caveolin-1 in the cancer cell and the stroma is unclear. In terms of prostatic stroma, caveolin-1 and cavin-1 expression has been examined in the prostate stroma cell line, PrSC,[13] and we also confirmed high expression of stromal caveolin-1 and cavin-1 in the TMA suggesting abundant caveolae in normal prostate stroma. Importantly, in contrast to the cancer cell where caveolin-1 is induced in advanced disease, loss of caveolin-1 expression in prostate cancer stroma correlates with prostate cancer progression and metastasis.[14] Here we provide the first evidence that stromal cavin-1 is also reduced in prostate cancer, compared with all benign stroma included in benign hyperplasia. The concomitant reduction of stromal caveolin-1 and cavin-1 suggests downregulation of stromal caveolae in prostate cancer. This is in stark contrast to the induction of non-caveolar caveolin-1 in advanced prostate cancer cells. These complex roles of caveolin-1 and caveolae between prostate epithelia (pro-tumor) and stroma (antitumor) highlight the limitations and difficulties in the therapeutic approach to caveolin-1 in advanced prostate cancer.

One of the most important targets in prostate cancer is the AR. Misregulated activation of AR has been associated with progression of advanced prostate cancer, and contributes to resistance to androgen deprivation therapy.[46] Caveolin-1 expression has been correlated with androgen deprivation therapy and castration resistance.[4,15] Proposed molecular mechanisms for caveolin-1 in castration-resistant prostate cancer include activation of the Akt pathway,[1,31] and an increase in the activity of AR in a low androgen environment.[46] Here we show that cavin-1 co-expression reversed planar caveolin-1-stimulated AR expression and specifically downregulated pAkt without affecting pERK. Co-ordinated inhibition of phosphatidylinositol-3-kinase and AR caused tumor regression,[47] hence further characterization of the molecular pathways activated by planar caveolin-1, and attenuated by cavin-1, may lead to novel therapeutic targets for caveolin-1-positive prostate cancer.

Previously, we showed attenuated secretion of IL-6 from cavin-1-expressing PC-3 cells.[12] Here, we report that cavin-1 expression correlates with a significant reduction in IL-6 levels in PC-3 xenograft tumors. Furthermore, using α-SMA as a marker for myofibroblasts, we found a significant reduction of reactive stroma in cavin-1-PC-3 tumors compared with control. IL-6 is a pleiotropic cytokine implicated in prostate cancer progression and a potential therapeutic target.[21,23] IL-6 in the tumor microenvironment has been reported to trigger activation of reactive stroma including fibroblasts and immune cells, also known as the efferent pathway (tumor cells stimulate mesenchymal–mesenchymal transition).[25,26] Furthermore, IL-6 is involved in the afferent pathway, where reactive stroma activates epithelial–mesenchymal transition.[26,27] The study also showed that coinjection of IL-6-stimulated human prostate fibroblast with PC-3 cells increased PC-3 *in vivo* tumor formation and lung metastases.[25] Although IL-6 functions as an autocrine growth factor for PC-3 cells, there have been conflicting results regarding IL-6 secretion from LNCaP cells.[32–34] In our study, IL-6 secretion was not detected in any of the LNCaP stable cell lines, but we found that LNCaP cells expressed IL-6, which was slightly but significantly increased by caveolin-1 expression. Expression of cavin-1 in LNCaP-caveolin-1 cells reduced IL-6 expression. However, as IL-6 is not secreted from any of the LNCaP cell lines, the functional significance of IL-6 regulation by caveolin-1 and cavin-1 in LNCaP cells remains unclear. Recent phase II trials report partial therapeutic efficacy of CNTO328 (siltuximab), anti-IL-6 monoclonal antibody, in castration-resistant prostate cancer.[21,23] In previous studies, anti-IL-6 therapy using CNTO328 inhibited the conversion of androgen-dependent to androgen-independent phenotype of prostate cancer in a mouse model.[21] Therefore, one possibility is that during the acquisition of androgen independence, prostate cancer cells acquire the ability to secretion IL-6.

In summary, the data presented in this work demonstrate differential expressions of caveolin-1 and cavin-1 in prostate carcinoma and stroma, and confirm a potential tumor-promoting role of non-caveolar caveolin-1 in advanced prostate cancer. Cavin-1 attenuates the effect of the pro-tumor caveolin-1 in the tumor microenvironment leading to suppression of tumor growth and metastasis. With the potential to identify caveolin-1-positive prostate cancers using circulating caveolin-1 as an accessible biomarker, this work establishes a new paradigm for research into targeted therapies for personalized cancer treatment.

MATERIALS AND METHODS

Reagents and antibodies

Xenolight D-luciferin potassium salt was from Thermo Fisher Scientific (Melbourne, VIC, Australia). Rabbit (610059) and mouse anti-caveolin-1 (610407) antibodies were acquired from BD Transduction Laboratories (Sydney, NSW, Australia), anti-β-actin (A1978) and anti-IL-6 (I2143) antibodies from Sigma-Aldrich (Sydney, NSW, Australia), anti-AR (1852–1) antibodies from Epitomics (DKSH, Melbourne, VIC, Australia), antibodies against phospho-Akt (9271), phospho-p44/42 MAPK (9106) and Akt (9272) from Cell Signaling Technology (Genesearch, Gold Coast, QLD, Australia), and anti-Erk2 (sc-154) and anti-human IL-6 (sc-7920) antibodies from Santa Cruz Biotechnology (Thermo Fisher Scientific). Rabbit anti-cavin-1 antibodies were produced against peptides comprising the N-terminal 15 amino acids of human cavin-1 and affinity purified. Anti-human Ki-67 (M7240) antibody was purchased from Dako (Melbourne, VIC, Australia) and anti-SMA (CM001C) antibody was acquired from Biocare Medical (Stafford, QLD, Australia).

Tissue microarray

TMAs were obtained from the Australian Prostate Cancer BioResource with human ethics approval from the University of Queensland (project number 2008002197). Sections were dewaxed and rehydrated through descending graded alcohols to running tap water and then washed in 2 changes of phosphate-buffered saline (PBS). Antigen retrieval was performed in 0.01 M Citric acid buffer, pH 6.0 at 105 °C for 15 min using Biocare Decloaking Chamber. After washing, endogenous peroxidase activity was blocked by incubating the sections in 3% H_2O_2 in PBS, and the slides were further blocked for 30 min in Biocare Medical Background Sniper (Biocare Medical, Stafford, QLD, Australia). Primary antibody incubation was performed overnight at room temperature in a humid chamber using the following conditions: rabbit anti-caveolin-1 was diluted 1:80 in PBS, rabbit anti-cavin-1 antibodies were diluted 1:50 in Renaissance antibody diluent (Biocare Medical). After washing in PBS, horseradish peroxidase coupled anti-rabbit antibody (Dako Envision Plus, Dako) was applied for 30 min. Color was developed by application of 3,3′ diaminobenzidine and H_2O_2 for 5 min and then excess chromogen was removed by washing in running tap water.

Sections were lightly counterstained in Mayers' hematoxylin, then dehydrated through ascending graded alcohols, cleared in xylene and mounted. Initial optimization experiments performed using Biocare Medical MACH3 Rabbit HRP polymer with caveolin antibody produced excessive background and were disregarded. Images were taken using Olympus BX41 microscope (OLYMPUS, Mt Waverley, VIC, Australia) using $\times 20$ objective in air with PixeLINK megapixel firewire 1394 camera (PixeLINK, Ottawa, ON, Canada).

Cell lines and stable sublines

Cervical cancer cell line HeLa, and prostate cancer cell lines PC-3 and LNCaP were purchased from American Type Culture Collection (ATCC, Manassas, VA, USA). Prostate cancer cell line 22Rv1 was a generous gift from Dr John Hooper (Mater Medical Research Institute, Brisbane, QLD, Australia). HeLa cells were maintained in Dulbecco's modified Eagle's medium (Invitrogen, Melbourne, VIC, Australia), and all prostate cancer cell lines were grown in RPMI-1640 (Invitrogen) medium supplemented with 10% fetal bovine serum in a humidified atmosphere of 5% CO_2 at 37 °C. Prostate cancer PC-3 cells expressing firefly luciferase were prepared as previously described in Luk *et al.*[18] To establish stable cell lines for cavin-1 expression, Gateway recombination cloning system (Life Technologies, Mulgrave, VIC, Australia) was used according to the manufacturer's instructions and as previously carried out by Skalamera *et al.*[48] Human cavin-1 was cloned into the lentivirus plasmid plv411 using forward primer 5′-GGGGACAAGTTTGTACAAAAAAGCAGGCTATGGAGGACCCCACGCTCTATA TTGTCG-3′ and reverse primer 5′-GGGGACCACTTTGTACAAGAAAGCTGGG TTCAGTCGCTGTCGCTCTTGTCC-3′ and verified by sequencing. Caveolin-1 plv411 was provided by ARVEC.[49] Lentiviral plv411 constructs were then packaged into lentiviruses for transduction into prostate cancer cells. Target cell lines were infected with lentiviruses in the presence of hexadimethrine bromide (8 μg/ml), then after 10 days, pure population of stable sublines expressing green fluorescent protein were selected by flow cytometry.

Immunoblotting

Total cells were lysed in a buffer containing 20 mM Tris pH 7.5, 150 mM NaCl, 0.5% Triton X-100, 0.5% deoxysodium cholate, 10 mM sodium fluoride (NaF), 0.5 mM sodium vanadate, 1 mM sodium pyrophosphate, 0.5 mM 4-(2-aminoethyl) benzenesulfonyl fluoride hydrochloride and protease inhibitors (1 μg/μl aprotinin, 1 μg/μl antipain, 1 μg/μl pepstatin, 1 μg/μl leupeptin and 2.5 mM benzamidine). Insoluble material was removed by centrifugation at 10 000 $\times g$ at 4 °C for 5 min, and protein concentration was determined using BCA assay (Thermo Fisher Scientific) following the manufacturer's instructions. Total cell lysate (20 μg) was diluted in sodium dodecyl sulfate–polyacrylamide gel electrophoresis sample buffer and boiled at 96 °C for 5 min. Proteins were resolved on sodium dodecyl sulfate–polyacrylamide gel electrophoresis gels and transferred on to polyvinylidene difluoride membranes. Membranes were blocked with 5% milk powder, and then incubated with primary antibodies; anti-cavin-1 (1:1000), anti-caveolin-1 (1:3000), anti-AR (1:1000) and anti-IL-6 (1:1000) overnight at 4 °C. Washed membranes were subsequently incubated with horseradish peroxidase-conjugated secondary antibody (Invitrogen) for 1 h at room temperature, and the signal was detected using SuperSignal West Pico chemiluminescence (Thermo Fisher Scientific).

Cell proliferation and anchorage-independent growth assays

PC-3 and LNCaP sublines were plated at a density of 5×10^4 cells per well, and 1×10^5 cells per well of 22Rv1 sublines were plated in six-well plates. Then, cell proliferation was measured by counting cells stained with Trypan blue using hemocytometer at day 2, 4 and 6. Anchorage-independent growth in soft agar was evaluated at day 21 after plating 10 000 cells per well in six-well plates between two layers of agarose, top layer being 0.35% and bottom layer 0.5%.

Immunofluorescence

LNCaP stables were grown on coverslips and fixed in cold methanol. Coverslips were washed three times with PBS and incubated with anti-caveolin-1 and anti-cavin-1 followed by their appropriate secondary antibodies with PBS washes in between. All antibodies were incubated for 1 h. Coverslips were mounted using ProLong Gold (Invitrogen), and visualized using a Zeiss Meta 510 confocal microscope (Carl Zeiss Pty Ltd, North Ryde, NSW, Australia).

Orthotopic prostate tumor xenograft study

The animal experiments described in this study were approved by the University of Queensland Animal Ethics Committee (UQDI/326/10/AICR). Seven-week-old male NOD.CB17-Prkdc^{scid} (severe combined immunodeficient, non-obese diabetic) mice were purchased from Animal Resource Centre (ARC, Perth, WA, Australia). Twenty-three mice were randomized into two groups, control PC-3 ($n = 11$) and PC-3-cavin-1 ($n = 12$). In all, 20 μl cell suspension containing 5×10^5 PC-3 cells in PBS were orthotopically xenografted into mouse dorsolateral prostate glands under a dissecting microscope. Primary tumor progression was monitored by *in vivo* whole-body bioluminescence. Before the imaging, D-luciferin dissolved in PBS was intraperitoneally injected, and then the bioluminescence was examined using the IVIS spectrum (Caliper Life Sciences, Mountain View, CA, USA). Prostate tumors were collected at the end of the experiment, and tumor weight and size were measured.

All mouse tissues were fixed in 10% buffered formalin for 24 h, and then 3 μm paraffin-embedded tissue sections were used for immunohistochemistry. Sections after deparaffinization and antigen retrieval were incubated with primary antibodies, including anti-Ki-67 (1:120 dilutions) and anti-SMA (1:800 dilutions) for 1 h at room temperature, and anti-IL-6 (1:50 dilutions) for overnight at 4 °C in a humidity chamber. Signals were developed in 3,3′ diaminobenzidine, and sections were lightly counterstained in Mayers' hematoxylin. Ki-67-positive cells at five arbitrarily selected fields from each tumor were counted at high-power field ($\times 400$ magnification) for the quantification of proliferating cells. Semiquantitative scoring for IL-6 and α-SMA was assessed as 0, 1+, 2+, 3+ and 4+, representing nil, weak, moderate, strong and the most intense staining, and data are presented as mean ± s.e.m. of five randomly selected microscopic fields from each tumor.

Statistical analysis

Experimental data were expressed as mean ± s.e.m. and statistical analyses were performed by two-tailed Student's *t*-test using GraphPad Prism 5 Software (GraphPad Software Inc, La Jolla, CA, USA). Significance was considered as P-value < 0.05.

CONFLICT OF INTEREST

The authors declare no conflict of interest.

ACKNOWLEDGEMENTS

We thank Duka Skalamera and Mareike Dahmer of the UQDI ARVEC facility for producing lentivirus, and the participants who kindly donated tissues to the Australian Prostate Cancer BioResource. This work was supported by project grants from the Association for International Cancer Research and Prostate Cancer Foundation Australia. MMH received a Career Development Award from the National Health and Medical Research Council of Australia (no. 569512). RGP was supported by NHMRC Project Grant 631371 and an NHMRC Australia Fellowship (569452). HM is supported by University of Queensland International Postgraduate Research Scholarship. The Australian Prostate Cancer BioResource is supported by an NHMRC Enabling Grant (no. 614296) and by an infrastructure grant from the Prostate Cancer Foundation of Australia. The ARVEC facility received support from the Australian Cancer Research Foundation.

REFERENCES

1 Li L, Ren CH, Tahir SA, Ren C, Thompson TC. Caveolin-1 maintains activated Akt in prostate cancer cells through scaffolding domain binding site interactions with and inhibition of serine/threonine protein phosphatases PP1 and PP2A. *Mol Cell Biol* 2003; **23**: 9389–9404.
2 Bryant KG, Camacho J, Jasmin JF, Wang C, Addya S, Casimiro MC *et al.* Caveolin-1 overexpression enhances androgen-dependent growth and proliferation in the mouse prostate. *Int J Biochem Cell Biol* 2011; **43**: 1318–1329.
3 Tahir SA, Yang G, Goltsov AA, Watanabe M, Tabata K, Addai J *et al.* Tumor cell-secreted caveolin-1 has proangiogenic activities in prostate cancer. *Cancer Res* 2008; **68**: 731–739.
4 Tahir SA, Yang G, Ebara S, Timme TL, Satoh T, Li L *et al.* Secreted caveolin-1 stimulates cell survival/clonal growth and contributes to metastasis in androgen-insensitive prostate cancer. *Cancer Res* 2001; **61**: 3882–3885.
5 Gumulec J, Sochor J, Hlavna M, Sztalmachova M, Krizkova S, Babula P *et al.* Caveolin-1 as a potential high-risk prostate cancer biomarker. *Oncol Rep* 2012; **27**: 831–841.

6 Tahir SA, Ren C, Timme TL, Gdor Y, Hoogeveen R, Morrisett JD *et al.* Development of an immunoassay for serum caveolin-1: a novel biomarker for prostate cancer. *Clin Cancer Res* 2003; **9**: 3653–3659.
7 Kuo SR, Tahir SA, Park S, Thompson TC, Coffield S, Frankel AE *et al.* Anti-caveolin-1 antibodies as anti-prostate cancer therapeutics. *Hybridoma* 2012; **31**: 77–86.
8 Parton RG, Simons K. The multiple faces of caveolae. *Nat Rev Mol Cell Biol* 2007; **8**: 185–194.
9 Hill MM, Bastiani M, Luetterforst R, Kirkham M, Kirkham A, Nixon SJ *et al.* PTRF-Cavin, a conserved cytoplasmic protein required for caveola formation and function. *Cell* 2008; **132**: 113–124.
10 Aung CS, Hill MM, Bastiani M, Parton RG, Parat MO. PTRF-cavin-1 expression decreases the migration of PC3 prostate cancer cells: role of matrix metalloprotease 9. *Eur J Cell Biol* 2011; **90**: 136–142.
11 Hill MM, Daud NH, Aung CS, Loo D, Martin S, Murphy S *et al.* Co-regulation of cell polarization and migration by caveolar proteins PTRF/Cavin-1 and caveolin-1. *PLoS One* 2012; **7**: e43041.
12 Inder KL, Zheng YZ, Davis MJ, Moon H, Loo D, Nguyen H *et al.* Expression of PTRF in PC-3 cells modulates cholesterol dynamics and the actin cytoskeleton impacting secretion pathways. *Mol Cell Proteomics* 2012; **11**(M111): 012245.
13 Gould ML, Williams G, Nicholson HD. Changes in caveolae, caveolin, and polymerase 1 and transcript release factor (PTRF) expression in prostate cancer progression. *Prostate* 2010; **70**: 1609–1621.
14 Di Vizio D, Morello M, Sotgia F, Pestell RG, Freeman MR, Lisanti MP. An absence of stromal caveolin-1 is associated with advanced prostate cancer, metastatic disease and epithelial Akt activation. *Cell Cycle* 2009; **8**: 2420–2424.
15 Yang G, Truong LD, Timme TL, Ren C, Wheeler TM, Park SH *et al.* Elevated expression of caveolin is associated with prostate and breast cancer. *Clin Cancer Res* 1998; **4**: 1873–1880.
16 Yang G, Truong LD, Wheeler TM, Thompson TC. Caveolin-1 expression in clinically confined human prostate cancer: a novel prognostic marker. *Cancer Res* 1999; **59**: 5719–5723.
17 Karam JA, Lotan Y, Roehrborn CG, Ashfaq R, Karakiewicz PI, Shariat SF. Caveolin-1 overexpression is associated with aggressive prostate cancer recurrence. *Prostate* 2007; **67**: 614–622.
18 Luk SU, Yap WN, Chiu YT, Lee DT, Ma S, Lee TK *et al.* Gamma-tocotrienol as an effective agent in targeting prostate cancer stem cell-like population. *Int J Cancer* 2011; **128**: 2182–2191.
19 Culig Z, Puhr M. Interleukin-6: a multifunctional targetable cytokine in human prostate cancer. *Mol Cell Endocrinol* 2012; **360**: 52–58.
20 Wu CT, Hsieh CC, Lin CC, Chen WC, Hong JH, Chen MF. Significance of IL-6 in the transition of hormone-resistant prostate cancer and the induction of myeloid-derived suppressor cells. *J Mol Med* 2012; **90**: 1343–1355.
21 Wallner L, Dai J, Escara-Wilke J, Zhang J, Yao Z, Lu Y *et al.* Inhibition of interleukin-6 with CNTO328, an anti-interleukin-6 monoclonal antibody, inhibits conversion of androgen-dependent prostate cancer to an androgen-independent phenotype in orchiectomized mice. *Cancer Res* 2006; **66**: 3087–3095.
22 Hudes G, Tagawa ST, Whang YE, Qi M, Qin X, Puchalski TA *et al.* A phase 1 study of a chimeric monoclonal antibody against interleukin-6, siltuximab, combined with docetaxel in patients with metastatic castration-resistant prostate cancer. *Invest New Drugs* 2013; **31**: 669–676.
23 Dorff TB, Goldman B, Pinski JK, Mack PC, Lara Jr PN, Van Veldhuizen Jr PJ *et al.* Clinical and correlative results of SWOG S0354: a phase II trial of CNTO328 (siltuximab), a monoclonal antibody against interleukin-6, in chemotherapy-pretreated patients with castration-resistant prostate cancer. *Clin Cancer Res* 2010; **16**: 3028–3034.
24 Nasu Y, Timme TL, Yang G, Bangma CH, Li L, Ren C *et al.* Suppression of caveolin expression induces androgen sensitivity in metastatic androgen-insensitive mouse prostate cancer cells. *Nat Med* 1998; **4**: 1062–1064.
25 Giannoni E, Bianchini F, Masieri L, Serni S, Torre E, Calorini L *et al.* Reciprocal activation of prostate cancer cells and cancer-associated fibroblasts stimulates epithelial-mesenchymal transition and cancer stemness. *Cancer Res* 2010; **70**: 6945–6956.
26 Hugo HJ, Lebret S, Tomaskovic-Crook E, Ahmed N, Blick T, Newgreen DF *et al.* Contribution of fibroblast and mast cell (afferent) and tumor (efferent) IL-6 effects within the tumor microenvironment. *Cancer Microenviron* 2012; **5**: 83–93.
27 Studebaker AW, Storci G, Werbeck JL, Sansone P, Sasser AK, Tavolari S *et al.* Fibroblasts isolated from common sites of breast cancer metastasis enhance cancer cell growth rates and invasiveness in an interleukin-6-dependent manner. *Cancer Res* 2008; **68**: 9087–9095.
28 Kalluri R, Zeisberg M. Fibroblasts in cancer. *Nat Rev Cancer* 2006; **6**: 392–401.
29 Mouraviev V, Li L, Tahir SA, Yang G, Timme TM, Goltsov A *et al.* The role of caveolin-1 in androgen insensitive prostate cancer. *J Urol* 2002; **168**: 1589–1596.
30 Lu ML, Schneider MC, Zheng Y, Zhang X, Richie JP. Caveolin-1 interacts with androgen receptor. A positive modulator of androgen receptor mediated transactivation. *J Biol Chem* 2001; **276**: 13442–13451.
31 Li L, Ren C, Yang G, Goltsov AA, Tabata K, Thompson TC. Caveolin-1 promotes autoregulatory, Akt-mediated induction of cancer-promoting growth factors in prostate cancer cells. *Mol Cancer Res* 2009; **7**: 1781–1791.
32 Okamoto M, Lee C, Oyasu R. Interleukin-6 as a paracrine and autocrine growth factor in human prostatic carcinoma cells in vitro. *Cancer Res* 1997; **57**: 141–146.
33 Chung TD, Yu JJ, Spiotto MT, Bartkowski M, Simons JW. Characterization of the role of IL-6 in the progression of prostate cancer. *Prostate* 1999; **38**: 199–207.
34 Smith PC, Hobisch A, Lin DL, Culig Z, Keller ET. Interleukin-6 and prostate cancer progression. *Cytokine Growth Factor Rev* 2001; **12**: 33–40.
35 Goetz JG, Lajoie P, Wiseman SM, Nabi IR. Caveolin-1 in tumor progression: the good, the bad and the ugly. *Cancer Metastasis Rev* 2008; **27**: 715–735.
36 Tahir SA, Frolov A, Hayes TG, Mims MP, Miles BJ, Lerner SP *et al.* Preoperative serum caveolin-1 as a prognostic marker for recurrence in a radical prostatectomy cohort. *Clin Cancer Res* 2006; **12**: 4872–4875.
37 Hansen CG, Bright NA, Howard G, Nichols BJ. SDPR induces membrane curvature and functions in the formation of caveolae. *Nat Cell Biol* 2009; **11**: 807–814.
38 McMahon KA, Zajicek H, Li WP, Peyton MJ, Minna JD, Hernandez VJ *et al.* SRBC/cavin-3 is a caveolin adapter protein that regulates caveolae function. *EMBO J* 2009; **28**: 1001–1015.
39 Bastiani M, Liu L, Hill MM, Jedrychowski MP, Nixon SJ, Lo HP *et al.* MURC/Cavin-4 and cavin family members form tissue-specific caveolar complexes. *J Cell Biol* 2009; **185**: 1259–1273.
40 Bai L, Deng X, Li Q, Wang M, An W, Deli A *et al.* Down-regulation of the cavin family proteins in breast cancer. *J Cell Biochem* 2012; **113**: 322–328.
41 Li X, Jia Z, Shen Y, Ichikawa H, Jarvik J, Nagele RG *et al.* Coordinate suppression of Sdpr and Fhl1 expression in tumors of the breast, kidney, and prostate. *Cancer Sci* 2008; **99**: 1326–1333.
42 Martinez R, Martin-Subero JI, Rohde V, Kirsch M, Alaminos M, Fernandez AF *et al.* A microarray-based DNA methylation study of glioblastoma multiforme. *Epigenetics* 2009; **4**: 255–264.
43 Xu XL, Wu LC, Du F, Davis A, Peyton M, Tomizawa Y *et al.* Inactivation of human SRBC, located within the 11p15.5-p15.4 tumor suppressor region, in breast and lung cancers. *Cancer Res* 2001; **61**: 7943–7949.
44 Aboulaich N, Vainonen JP, Stralfors P, Vener AV. Vectorial proteomics reveal targeting, phosphorylation and specific fragmentation of polymerase I and transcript release factor (PTRF) at the surface of caveolae in human adipocytes. *Biochem J* 2004; **383**: 237–248.
45 Goetz JG, Minguet S, Navarro-Lerida I, Lazcano JJ, Samaniego R, Calvo E *et al.* Biomechanical remodeling of the microenvironment by stromal caveolin-1 favors tumor invasion and metastasis. *Cell* 2011; **146**: 148–163.
46 Bennett N, Hooper JD, Lee CS, Gobe GC. Androgen receptor and caveolin-1 in prostate cancer. *IUBMB Life* 2009; **61**: 961–970.
47 Carver BS, Chapinski C, Wongvipat J, Hieronymus H, Chen Y, Chandarlapaty S *et al.* Reciprocal feedback regulation of PI3K and androgen receptor signaling in PTEN-deficient prostate cancer. *Cancer Cell* 2011; **19**: 575–586.
48 Skalamera D, Ranall MV, Wilson BM, Leo P, Purdon AS, Hyde C *et al.* A high-throughput platform for lentiviral overexpression screening of the human ORFeome. *PLoS One* 2011; **6**: e20057.
49 Skalamera D, Dahmer M, Purdon AS, Wilson BM, Ranall MV, Blumenthal A *et al.* Generation of a genome scale lentiviral vector library for EF1alpha promoter-driven expression of human ORFs and identification of human genes affecting viral titer. *PLoS One* 2012; **7**: e51733.

Supplementary Information accompanies this paper on the Oncogene website (http://www.nature.com/onc)